

## 1D and 2D Homochiral Metal-Organic Frameworks Built from a New Chiral Elongated Binaphthalene-Derived Bipyridine

Chuan-De Wu, Lin Zhang, and Wenbin Lin\*

Department of Chemistry, CB#3290, University of North Carolina,  
Chapel Hill, North Carolina 27599

Received May 22, 2006

Six homochiral coordination polymers **1–6** based on a new enantiopure elongated (*S*)-2,2'-diethoxy-1,1'-binaphthyl-6,6'-bis(4-vinylpyridine) ligand (**L**) and divalent metal (Zn, Cd, and Ni) connecting points were synthesized and characterized by single-crystal X-ray diffraction studies. These new homochiral coordination polymers adopt two distinct framework structures: a one-dimensional infinite chain structure with bridging **L** ligands occupying the axial positions of the metal centers and a two-dimensional rhombic grid structure formed by linking octahedrally coordinated metal centers with four pyridyl groups of bridging **L** ligands in the equatorial positions. The structures of these coordination polymers are sensitive to the nature of the anions as well as the solvents from which the coordination polymer crystals were grown. Powder X-ray diffraction studies showed that the two-dimensional chiral rhombic grids exhibited porosity, which could potentially find applications in enantioselective separations and catalysis.

### Introduction

There is much current interest in the design and synthesis of new functional porous metal-organic frameworks (MOFs), which can be readily obtained by linking molecular building blocks via metal-coordination-driven self-assembly processes.<sup>1</sup> The interest in these species is in part fueled by their size- and shape-selective properties, which make them potentially useful in catalysis,<sup>2</sup> gas storage,<sup>3</sup> separation processes,<sup>4</sup> ion exchange,<sup>5</sup> and sensing devices.<sup>6</sup> Recent results clearly show that the crystal engineering of MOFs with predictable porous topological architectures can be achieved by connecting judiciously tailored building blocks.<sup>7</sup>

\* Author to whom correspondence should be addressed. Phone: (919) 962-6320. Fax: (919) 962-2388. E-mail: wlin@unc.edu.

- (1) (a) Piguet, C.; Bünnli, J.-C. *G. Chem. Soc. Rev.* **1999**, 28, 347. (b) Moulton, B.; Zaworotko, M. *J. Chem. Rev.* **2001**, 101, 1629. (c) Eddaoudi, M.; Moler, D. B.; Li, H.; Chen, B.; Reineke, T. M.; O'Keeffe, M.; Yaghi, O. M. *Acc. Chem. Res.* **2001**, 34, 319. (d) Evans, O. R.; Lin, W. *Acc. Chem. Res.* **2002**, 35, 511. (e) Janiak, C. *J. Chem. Soc., Dalton Trans.* **2003**, 2781. (f) Kitagawa, S.; Kitaura, R.; Noro, S. *Angew. Chem., Int. Ed.* **2004**, 43, 2334. (g) Oh, M.; Carpenter, G. B.; Sweigart, D. A. *Acc. Chem. Res.* **2004**, 37, 1. (h) James, S. L. *Chem. Soc. Rev.* **2003**, 32, 276.
- (2) (a) Fujita, M.; Kwon, Y.-J.; Washizu, S.; Ogura, K. *J. Am. Chem. Soc.* **1994**, 116, 1151. (b) Seo, J. S.; Wand, D.; Lee, H.; Jun, S. I.; Oh, J.; Jeon, Y.; Kim, K. *Nature* **2000**, 404, 982. (c) Sawaki, T.; Aoyma, Y. *J. Am. Chem. Soc.* **1999**, 121, 4793. (d) Kesani, B.; Lin, W. *Coord. Chem. Rev.* **2003**, 246, 305. (e) Hu, A.; Ngo, H. L.; Lin, W. *J. Am. Chem. Soc.* **2003**, 125, 11490. (f) Wu, C.-D.; Hu, A.; Zhang, L.; Lin, W. *J. Am. Chem. Soc.* **2005**, 127, 8940. (g) Cho, S.-H.; Ma, B.; Nguyen, S. T.; Hupp, J. T.; Albrecht-Schmitt, T. E. *Chem. Commun.* **2006**, 2563.

Bipyridine-type ligands, Py–X–Py (Py = pyridyl and spacer X = functional group, such as,  $-\text{CH}_2\text{CH}_2-$ ,<sup>8</sup>  $-\text{CH}=\text{CH}-$ ,<sup>9</sup>  $-\text{C}\equiv\text{C}-$ ,<sup>10</sup>  $-\text{N}=\text{N}-$ ,<sup>11</sup> phenyl and biphenyl,<sup>12</sup> and others<sup>13</sup>), have been widely used as effective linkers in the synthesis of a variety of MOFs. Bipyridine-type ligands are convenient neutral linkers for the crystal engineering of desired MOFs by modification of the spacer X. The porosity, functionality, and chirality of the resulting MOFs can be

- (3) (a) Noro, S.; Kitagawa, S.; Kondo, M.; Seki, K. *Angew. Chem., Int. Ed.* **2000**, 39, 2081. (b) Seki, K.; Mori, W. *J. Phys. Chem. B* **2002**, 106, 1380. (c) Rosi, N. L.; Eckert, J.; Eddaoudi, M.; Vodak, D. T.; Kim, J.; O'Keeffe, M.; Yaghi, O. M. *Science* **2003**, 300, 1127. (d) Férey, G.; Latroche, M.; Serre, C.; Millange, F.; Loiseau, T.; Percheron-Guégan, A. *Chem. Commun.* **2003**, 2976. (e) Kesani, B.; Cui, Y.; Smith, M.; Bittner, E.; Bockrath, B.; Lin, W. *Angew. Chem., Int. Ed.* **2005**, 44, 72.
- (4) (a) Min, K. S.; Suh, M. P. *Chem.—Eur. J.* **2001**, 7, 303. (b) Uemura, K.; Kitagawa, S.; Kondo, M.; Fukui, K.; Kitaura, R.; Chang, H.-C.; Mizutani, T. *Chem.—Eur. J.* **2002**, 8, 3586. (c) Suh, M. P.; Ko, J. W.; Choi, H. J. *J. Am. Chem. Soc.* **2002**, 124, 10976. (d) Kitaura, R.; Seki, K.; Akiyama, G.; Kitagawa, S. *Angew. Chem., Int. Ed.* **2003**, 42, 428. (e) Bradshaw, D.; Prior, T. J.; Cussen, E. J.; Claridge, J. B.; Rosseinsky, M. J. *J. Am. Chem. Soc.* **2004**, 126, 6106.
- (5) (a) Hoskins, B. F.; Robson, R. *J. Am. Chem. Soc.* **1990**, 112, 1546. (b) Min, K. S.; Suh, M. P. *J. Am. Chem. Soc.* **2000**, 122, 6834. (c) Yaghi, O. M.; Li, H. *J. Am. Chem. Soc.* **1996**, 118, 295.
- (6) (a) Albrecht, M.; Lutz, M.; Spek, A. L.; van Koten, G. *Nature* **2000**, 406, 970. (b) Real, J. A.; Andrés, E.; Muñoz, M. C.; Julve, M.; Granier, T.; Boussekou, A.; Varret, F. *Science* **1995**, 268, 265. (c) Beauvais, L. G.; Shores, M. P.; Long, J. R. *J. Am. Chem. Soc.* **2000**, 122, 2763.
- (7) Kitaura, R.; Kitagawa, S.; Kubota, Y.; Kobayashi, T. C.; Kindo, K.; Mita, Y.; Matsuo, A.; Kobayashi, M.; Chang, H. C.; Ozawa, T. C.; Suzuki, M.; Sakata, M.; Takata, M. *Science* **2002**, 298, 2358.

controlled by tuning the spacer X.<sup>14</sup> We have recently explored the incorporation of readily available 1,1'-binaphthol and its derivatives as the key functional groups (X) in a variety of bridging ligands.<sup>15</sup> Such a strategy has led to novel catalytically active MOFs.<sup>2f</sup> To better understand the factors that govern the crystal growth via metal-coordination-driven self-assembly processes, we have explored the design and synthesis of homochiral MOFs using chiral binaphthalene-derived bipyridines of diverse lengths, shapes, and functionalities. This work reports the synthesis and characterization of a family of homochiral solids built from a new enantiopure elongated (*S*)-2,2'-diethoxy-1,1'-binaphthyl-6,6'-bis(4-vinylpyridine) ligand (**L**) and divalent metal (Zn, Cd, and Ni) connecting points. These new homochiral coordination

- (8) (a) Lu, J. Y.; Babb, A. *Inorg. Chim. Acta* **2001**, *318*, 186. (b) Hernandez, M. L.; Barandika, M. G.; Urtiaga, M. K.; Cortes, R.; Lezama, L.; Arriortua, M. I.; Rojo, T. *Dalton Trans.* **1999**, 1401. (c) Sain, S.; Maji, T. K.; Mostafa, G.; Lu, T.-H.; Chaudhuri, N. R. *New J. Chem.* **2003**, *27*, 185. (d) Suresh, E.; Bhadbhade, M. M. *CrystEngComm* **2001**, *13*. (e) Plater, M. J.; Foreman, M. R. S. J.; Skakle, J. M. S. *Cryst. Eng.* **2001**, *4*, 293. (f) Ferbinteanu, M.; Marinescu, G.; Roesky, H. W.; Noltemeyer, M.; Schmidt, H.-G.; Andruh, M. *Polyhedron* **1999**, *18*, 243. (g) Carlucci, L.; Ciani, G.; Proserpio, D. M.; Rizzato, S. *Chem. Commun.* **2000**, 1319. (h) Hennigar, T. L.; MacQuarrie, D. C.; Losier, P.; Rogers, R. D.; Zaworotko, M. J. *Angew. Chem., Int. Ed. Engl.* **1997**, *36*, 972.
- (9) (a) Knaust, J. M.; Keller, S. W. *Inorg. Chem.* **2002**, *41*, 5650. (b) Jung, O.-S.; Park, S. H.; Kim, K. M.; Jang, H. G. *Inorg. Chem.* **1998**, *37*, 5781. (c) Lu, J. Y.; Norman, C. *Polyhedron* **2003**, *22*, 235. (d) Batten, S. R.; Hoskins, B. F.; Robson, R. *Chem.—Eur. J.* **2000**, *6*, 156. (e) Munno, G. D.; Cipriani, F.; Armentano, D.; Julve, M.; Real, J. A. *New J. Chem.* **2001**, *25*, 1031. (f) Lu, J. Y.; Runnels, K. A.; Norman, C. *Inorg. Chem.* **2001**, *40*, 4516. (g) Real, J. A.; Andres, E.; Munoz, M. C.; Julve, M.; Granier, T.; Bousseksou, A.; Varret, F. *Science* **1995**, *268*, 265.
- (10) (a) Carlucci, L.; Ciani, G.; Proserpio, D. M. *Dalton Trans.* **1999**, 1799. (b) Dong, Y.-B.; Layland, R. C.; Pschirer, N. G.; Smith, M. D.; Bunz, U. H. F.; Loya, H.-C. z. *Chem. Mater.* **1999**, *11*, 1413. (c) Carlucci, L.; Ciani, G.; Macchi, P.; Proserpio, D. M. *Chem. Commun.* **1998**, 1837. (d) Carlucci, L.; Ciani, G.; Proserpio, D. M. *Chem. Commun.* **1999**, 449. (e) Dong, Y.-B.; Layland, R. C.; Smith, M. D.; Pschirer, N. G.; Bunz, U. H. F.; Loya, H.-C. z. *Inorg. Chem.* **1999**, *38*, 3056.
- (11) (a) Kondo, M.; Shimamura, M.; Noro, S.-I.; Minakoshi, S.; Asami, A.; Seki, K.; Kitagawa, S. *Chem. Mater.* **2000**, *12*, 1288. (b) Carlucci, L.; Ciani, G.; Proserpio, D. M. *Dalton Trans.* **1999**, 1799. (c) Withersby, M. A.; Blake, A. J.; Champness, N. R.; Cooke, P. A.; Hubberstey, P.; Schroder, M. *New J. Chem.* **1999**, *23*, 573. (d) Halder, G. J.; Kepert, C. J.; Moubaraki, B.; Murray, K. S.; Cashion, J. D. *Science* **2002**, 298, 1762. (e) Li, B.; Yin, G.; Cao, H.; Liu, Y.; Xu, Z. *Inorg. Chem. Commun.* **2001**, *4*, 451. (f) Li, B.; Lang, J.; Ding, J.; Zhang, Y. *Inorg. Chem. Commun.* **2003**, *6*, 141. (g) Withersby, M. A.; Blake, A. J.; Champness, N. R.; Cooke, P. A.; Hubberstey, P.; Realf, A. L.; Teat, S. J.; Schroder, M. *Dalton Trans.* **2000**, 3261. (h) He, C.; Zhang, B.-G.; Duan, C.-Y.; Li, J.-H.; Meng, Q.-J. *Eur. J. Inorg. Chem.* **2000**, 2549.
- (12) (a) Biradha, K.; Fujita, M. *Dalton Trans.* **2002**, 3805. (b) Herbstein, F. H.; Hu, S.; Kapon, M. *Acta Crystallogr., Sect. B* **2002**, *58*, 884. (c) Biradha, K.; Hongo, Y.; Fujita, M. *Angew. Chem., Int. Ed.* **2000**, *39*, 3843. (d) Biradha, K.; Hongo, Y.; Fujita, M. *Angew. Chem., Int. Ed.* **2002**, *41*, 3395. (e) Biradha, K.; Fujita, M. *Chem. Commun.* **2001**, *15*. (f) Biradha, K.; Fujita, M. *Chem. Commun.* **2002**, 1866.
- (13) (a) Zheng, N.; Bu, X.; Feng, P. *J. Am. Chem. Soc.* **2002**, *124*, 9688. (b) Hamilton, T. D.; Papaefstathiou, G. S.; MacGillivray, L. R. *J. Am. Chem. Soc.* **2002**, *124*, 11606. (c) Papaefstathiou, G. S.; MacGillivray, L. R. *Angew. Chem., Int. Ed.* **2002**, *41*, 2070. (d) Kitaura, R.; Fujimoto, K.; Noro, S.; Kondo, M.; Kitagawa, S. *Angew. Chem., Int. Ed.* **2002**, *41*, 133. (e) Biradha, K.; Fujita, M. *Dalton Trans.* **2000**, 3805. (f) Loi, M.; Graf, E.; Hosseini, M. W.; Cian, A. D.; Fischer, J. *Chem. Commun.* **1999**, 603. (g) Ciurtin, D. M.; Pschirer, N. G.; Smith, M. D.; Bunz, U. H. F.; zur Loya, H.-C. *Chem. Mater.* **2001**, *13*, 2743.
- (14) Pschirer, N. G.; Ciurtin, D. M.; Smith, M. D.; Bunz, U. H. F.; zur Loya, H.-C. *Angew. Chem., Int. Ed.* **2002**, *41*, 583.
- (15) (a) Cui, Y.; Ngo, H. L.; Lin, W. *Chem. Commun.* **2003**, 1388. (b) Wu, C.-D.; Ngo, H. L.; Lin, W. *Chem. Commun.* **2004**, 1588. (c) Cui, Y.; Lee, S. J.; Lin, W. *J. Am. Chem. Soc.* **2003**, *125*, 6014.

polymers adopt either a one-dimensional infinite chain structure with bridging **L** ligands occupying the axial positions of the metal centers or a two-dimensional rhombic grid structure formed by linking octahedrally coordinated metal centers with four pyridyl groups of bridging **L** ligands in the equatorial positions.

## Experimental Section

**Materials and Methods.** All of the chemicals were purchased from Aldrich or Fisher Scientific and used without further purification. The infrared (IR) spectra were recorded as KBr pellets on a Nicolet Magna-560 Fourier transform infrared spectrometer. X-ray powder diffraction data were recorded on a Rigaku MultiFlex diffractometer at 40 kV and 40 mA for Cu K $\alpha$  ( $\lambda = 1.5406 \text{ \AA}$ ), with a scan speed of 0.5°/min. Thermogravimetric analysis (TGA) experiments were carried out at a heating rate of 4 °C/min in air with a Shimadzu TGA-50 thermogravimetric analyzer.

**Synthesis of 6,6'-Dichloro-2,2'-diethoxy-1,1'-binaphthyl-4,4'-bis(4-vinylpyridine) (**L**).** A mixture of 4,4'-dibromo-6,6'-dichloro-2,2'-diethoxy-1,1'-binaphthyl (1.75 g, 3.1 mmol), 4-vinylpyridine (1.16 mL, 10.8 mmol), Pd(OAc)<sub>2</sub> (35 mg), and tris(*o*-tolyl)-phosphine (35 mg) in 12 mL of NEt<sub>3</sub> and 12 mL of *N,N*-dimethylformamide (DMF) was refluxed for 48 h. The mixture was allowed to cool to room temperature and then quenched with water. The volatiles were removed under reduced pressure, and the residue was dissolved in dichloromethane and washed with water three times. After drying over MgSO<sub>4</sub>, the solvent was removed under reduced pressure to afford a crude product which was purified by silica gel column chromatography using hexanes, ethyl acetate, and triethylamine (1:4:1 v/v) to give pure solid **L**. Yield: 73.7%. <sup>1</sup>H NMR (CDCl<sub>3</sub>, 400 MHz): δ 8.66 (d,  $J = 6.0 \text{ Hz}$ , 2H), 8.13 (s, 1H), 8.05 (d,  $J = 16 \text{ Hz}$ , 1H), 7.67 (s, 1H), 7.48 (d,  $J = 6.0 \text{ Hz}$ , 2H), 7.22 (dd,  $J = 1.6 \text{ Hz}$  and  $J = 9.2 \text{ Hz}$ , 1H), 7.10 (d,  $J = 16.0 \text{ Hz}$ , 1H), 4.12 (m, 2H), 1.10 (t,  $J = 6.8 \text{ Hz}$ , 3H). <sup>13</sup>C{<sup>1</sup>H} NMR (CDCl<sub>3</sub>, 400 MHz): δ 154.14, 150.23, 144.34, 134.61, 132.61, 130.11, 129.84, 129.71, 127.83, 127.58, 127.31, 122.63, 121.07, 114.18, 65.16, 14.92.

**Synthesis of [ZnL(DMF)<sub>4</sub>][ZnL(DMF)<sub>2</sub>(H<sub>2</sub>O)(ClO<sub>4</sub>)<sub>2</sub>·2DMF·EtOH·2H<sub>2</sub>O (**1**).** The slow diffusion of Et<sub>2</sub>O into a mixture of Zn(ClO<sub>4</sub>)<sub>2</sub>·6H<sub>2</sub>O (3.7 mg, 0.01 mmol), **L** (5.7 mg, 0.01 mmol) in a mixed solvent of DMF (0.5 mL), CHCl<sub>3</sub> (1 mL), and EtOH (1 mL) at room temperature afforded colorless crystals of **1** after 2 weeks. The crystals were filtered, washed with EtOH and Et<sub>2</sub>O, and dried at room temperature. Yield: 5.1 mg (41.7%). IR (KBr pellet,  $\nu/\text{cm}^{-1}$ ): 3483br, 3088w, 2927w, 1651s, 1614s, 1579m, 1503w, 1436w, 1373m, 1329m, 1202w, 1009s, 964w, 872w, 811w, 668w, 625m, 575w, 506w.

**Synthesis of [CdL(DMF)<sub>4</sub>][CdL(DMF)<sub>3</sub>(ClO<sub>4</sub>)<sub>2</sub>·2DMF (**2**).** The slow diffusion of Et<sub>2</sub>O into a mixture of Cd(ClO<sub>4</sub>)<sub>2</sub>·6H<sub>2</sub>O (4.2 mg, 0.01 mmol), **L** (5.7 mg, 0.01 mmol) in a mixed solvent of DMF (0.5 mL), CHCl<sub>3</sub> (1 mL), and EtOH (1 mL) afforded colorless crystals of **2** after 2 weeks. The crystalline product was filtered, washed with EtOH and Et<sub>2</sub>O, and dried at room temperature. Yield: 5.6 mg (44.5%). IR (KBr pellet,  $\nu/\text{cm}^{-1}$ ): 3430br, 2976w, 1663s, 1606s, 1579m, 1495w, 1429w, 1373w, 1329m, 1223m, 1206w, 1100s, 1017w, 968w, 923w, 878m, 811m, 768w, 662w, 627s, 549w, 509w.

**Synthesis of [CdL(H<sub>2</sub>O)(NO<sub>3</sub>)<sub>2</sub>][CdL(H<sub>2</sub>O)<sub>2</sub>(NO<sub>3</sub>)<sub>2</sub>·MeOH (**3**).** A mixture of Cd(NO<sub>3</sub>)<sub>2</sub>·4H<sub>2</sub>O (3.1 mg, 0.01 mmol), **L** (5.7 mg, 0.01 mmol), C<sub>6</sub>H<sub>4</sub>Cl<sub>2</sub> (1 mL), and MeOH (1 mL) in a capped vial was heated at 70 °C for 1 week. Colorless crystals of **3** were filtered, washed with MeOH and Et<sub>2</sub>O, and dried at room temperature. Yield: 3.9 mg (43.5%). IR (KBr pellet,  $\nu/\text{cm}^{-1}$ ): 3430br,

**Table 1.** Crystal Data and Structure Refinement for  $[ZnL(DMF)_4][ZnL(DMF)_2(H_2O)(ClO_4)_4 \cdot 3ClO_4 \cdot 2DMF \cdot EtOH \cdot 2H_2O$  (**1**),  $[CdL(DMF)_4][CdL(DMF)_3(ClO_4)_4 \cdot 3ClO_4 \cdot 2DMF$  (**2**),  $[CdL(H_2O)(NO_3)_2] \cdot [CdL(H_2O)_2(NO_3)_2] \cdot MeOH$  (**3**),  $[CdL_2(DMF)(H_2O)][CdL_2(H_2O)(ClO_4)_4 \cdot 3ClO_4 \cdot DMF \cdot 3CH_3CN \cdot 6H_2O$  (**4**),  $[CdL_2(NO_3)_2] \cdot DMF \cdot 2EtOH \cdot 2.5H_2O$  (**5**), and  $[NiL_2Cl_2] \cdot DMF \cdot 4EtOH \cdot H_2O$  (**6**)

	<b>1</b>	<b>2</b>	<b>3</b>
formula	$C_{102}H_{128}Cl_8N_{12}O_{32}Zn_2$	$C_{103}H_{123}Cd_2Cl_8N_{13}O_{29}$	$C_{77}H_{70}Cd_2Cl_4N_8O_{20}$
fw	2448.50	2515.54	1794.01
cryst size (mm <sup>3</sup> )	0.8 × 0.3 × 0.3	0.8 × 0.5 × 0.5	0.8 × 0.6 × 0.5
cryst color	colorless	colorless	colorless
cryst syst, space group	triclinic, <i>P</i> 1	triclinic, <i>P</i> 1	monoclinic, <i>P</i> 2 <sub>1</sub>
<i>a</i> (Å)	11.137(2)	11.151(2)	9.1608(2)
<i>b</i> (Å)	15.470(2)	15.498(2)	19.3673(4)
<i>c</i> (Å)	17.573(3)	17.514(4)	24.6754(5)
$\alpha$ (deg)	83.056(2)	82.93(2)	90
$\beta$ (deg)	88.764(2)	89.19(3)	98.143(1)
$\gamma$ (deg)	87.531(2)	87.64(3)	90
volume (Å <sup>3</sup> )	3002.2(7)	3001.1(9)	4333.77(16)
<i>Z</i>	1	1	2
calcd density (g cm <sup>-3</sup> )	1.354	1.392	1.375
F(000)	1276	1296	1824
abs coeff (mm <sup>-1</sup> )	0.655	0.608	0.683
$\theta$ for data collection (deg)	1.33–23.30	1.87–23.39	2.50–25.03
reflns collected ( <i>R</i> <sub>int</sub> )	13 611 (0.032)	34 805 (0.038)	45 765 (0.094)
data/params	12 558/1242	16 289/1372	15 197/970
goodness of fit on F <sup>2</sup>	1.042	1.051	1.066
R1 (wR2) [ <i>I</i> > 2σ( <i>I</i> )] <sup>a</sup>	0.1096 (0.2740)	0.0704 (0.1856)	0.0928 (0.2133)
flack param	0.11(3)	-0.02(3)	0.05(4)
largest diff. peak and hole (e Å <sup>3</sup> )	1.915 and -0.540	1.171 and -0.651	1.019 and -0.531
	<b>4</b>	<b>5</b>	<b>6</b>
formula	$C_{164}H_{159}Cd_2Cl_{12}N_{13}O_{34}$	$C_{83}H_{84}CdCl_4N_7O_{15.5}$	$C_{87}H_{93}Cl_6N_5NiO_{10}$
fw	3506.24	1681.77	1640.07
cryst size (mm <sup>3</sup> )	0.8 × 0.6 × 0.4	0.80 × 0.60 × 0.30	0.8 × 0.6 × 0.5
cryst color	colorless	colorless	light green
cryst syst, space group	triclinic, <i>P</i> 1	monoclinic, <i>C</i> 2	monoclinic, <i>C</i> 2
<i>a</i> (Å)	10.499(2)	27.796(8)	27.1399(9)
<i>b</i> (Å)	20.587(3)	31.895(11)	31.3132(8)
<i>c</i> (Å)	21.993(3)	10.176(3)	10.8308(8)
$\alpha$ (deg)	98.545(2)	90	90
$\beta$ (deg)	92.312(3)	103.40(3)	99.655(4)
$\gamma$ (deg)	100.165(2)	90	90
volume (Å <sup>3</sup> )	4616.0(12)	8776(5)	9074.0(8)
<i>Z</i>	1	4	4
calcd density (g cm <sup>-3</sup> )	1.261	1.273	1.201
F(000)	1806	3484	3440
abs coeff (mm <sup>-1</sup> )	0.473	0.435	0.446
$\theta$ for data collection (deg)	1.88–25.09	1.97–23.33	1.91–23.26
reflns collected ( <i>R</i> <sub>int</sub> )	69 517 (0.067)	34 151 (0.052)	36 748 (0.068)
data/params	30 619/1901	12 421/937	12 450/905
goodness of fit on F <sup>2</sup>	1.087	1.050	1.033
R1 (wR2) [ <i>I</i> > 2σ( <i>I</i> )] <sup>a</sup>	0.0930 (0.2151)	0.0940 (0.2398)	0.0953 (0.2439)
flack param	0.05(3)	0.01(4)	-0.01(3)
largest diff. peak and hole (e Å <sup>3</sup> )	1.245 and -0.828	2.160 and -0.690	0.892 and -0.770

$$^a R1 = \sum(|F_o| - |F_c|)/\sum|F_o|, wR2 = [\sum w(F_o^2 - F_c^2)^2 / \sum w(F_o^2)]^{0.5}$$

2978w, 1608s, 1579m, 1456s, 1373m, 1328m, 1287m, 1224m, 1206w, 1128m, 1086w, 1020m, 962w, 929w, 873w, 815m, 768w, 632w, 550w, 509w.

**Synthesis of  $[CdL_4(DMF)(ClO_4)(H_2O)_2] \cdot (ClO_4)_3 \cdot DMF \cdot 3CH_3CN \cdot 6H_2O$  (**4**)**. The slow diffusion of Et<sub>2</sub>O into a mixture of Cd(ClO<sub>4</sub>)<sub>2</sub>·6H<sub>2</sub>O (4.2 mg, 0.01 mmol), **L** (5.7 mg, 0.01 mmol) in a mixed solvent of DMF (0.5 mL), CHCl<sub>3</sub> (1 mL), and CH<sub>3</sub>CN (1 mL) afforded colorless crystals of **4** after 2 weeks. The crystalline product was filtered, washed with EtOH and Et<sub>2</sub>O, and dried at room temperature. Yield: 4.9 mg (55.9%). IR (KBr pellet, ν/cm<sup>-1</sup>):

3428br, 2978w, 2931w, 1650s, 1608s, 1578s, 1493m, 1430m, 1373m, 1329s, 1224m, 1205m, 1098s, 1060s, 966w, 926w, 872w, 810m, 771w, 718w, 670w, 622m, 533w, 510w.

**Synthesis of  $[CdL_2(NO_3)_2] \cdot DMF \cdot 2EtOH \cdot 2.5H_2O$  (**5**)**. The slow diffusion of Et<sub>2</sub>O into a mixture of Cd(NO<sub>3</sub>)<sub>2</sub>·4H<sub>2</sub>O (3.1 mg, 0.01 mmol) and **L** (5.7 mg, 0.01 mmol) in a mixed solvent of DMF (0.5 mL), CHCl<sub>3</sub> (1 mL), and EtOH (1 mL) afforded colorless

crystals of **5** after 3 days. The crystalline product was filtered, washed with EtOH and Et<sub>2</sub>O, and dried at room temperature. Yield: 3.7 mg (44.0% based on **L**). IR (KBr pellet, ν/cm<sup>-1</sup>): 3441br, 2979w, 1652m, 1608s, 1578m, 1432m, 1384s, 1329m, 1296m, 1223m, 1205w, 1126w, 1096m, 1059w, 1019w, 962w, 927w, 874w, 816m, 768w, 631w, 534w, 505w.

**Synthesis of  $[NiL_2Cl_2] \cdot DMF \cdot 4EtOH \cdot H_2O$  (**6**)**. The slow diffusion of Et<sub>2</sub>O into a mixture of NiCl<sub>2</sub>·6H<sub>2</sub>O (2.4 mg, 0.01 mmol) and **L** (5.7 mg, 0.01 mmol) in a mixed solvent of DMF (0.5 mL), CHCl<sub>3</sub> (1 mL), and EtOH (1 mL) afforded light green crystals of **6** after 5 days. The crystalline product was filtered, washed with EtOH and Et<sub>2</sub>O, and dried at room temperature. Yield: 3.5 mg (42.7% based on **L**). IR (KBr pellet, ν/cm<sup>-1</sup>): 3421, 2976w, 1670s, 1607s, 1578s, 1493m, 1455w, 1424w, 1372m, 1328s, 1221m, 1205m, 1168w, 1144w, 1125m, 1095w, 1059m, 1015w, 959w, 926w, 868m, 810s, 768w, 750m, 658w, 632m, 535w, 508m.

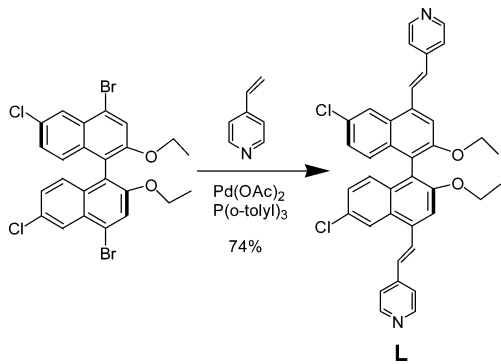
**Table 2.** Selected Bond Lengths [Å] and Angles [deg] for Compounds 1–6

1					
Zn(1)–N(2) <sup>a</sup>	2.278(14)	N(2) <sup>a</sup> –Zn(1)–O(3)	93.7(7)	N(8) <sup>a</sup> –Zn(2)–N(7)	174.0(9)
Zn(1)–O(3)	2.291(18)	N(2) <sup>a</sup> –Zn(1)–O(4)	89.5(6)	N(8) <sup>a</sup> –Zn(2)–O(12)	85.2(8)
Zn(1)–O(4)	2.292(15)	O(3)–Zn(1)–O(4)	93.7(6)	N(7)–Zn(2)–O(12)	92.6(7)
Zn(1)–O(5)	2.313(15)	N(2) <sup>a</sup> –Zn(1)–O(5)	89.3(6)	N(8) <sup>a</sup> –Zn(2)–O(10)	88.1(7)
Zn(1)–N(1)	2.363(15)	O(3)–Zn(1)–O(5)	170.3(6)	N(7)–Zn(2)–O(10)	94.0(6)
Zn(1)–O(6)	2.362(18)	O(4)–Zn(1)–O(5)	95.6(5)	O(12)–Zn(2)–O(10)	173.1(7)
Zn(2)–N(8) <sup>i</sup>	2.213(16)	N(2) <sup>a</sup> –Zn(1)–N(1)	178.2(7)	N(8) <sup>a</sup> –Zn(2)–O(11)	91.1(8)
Zn(2)–N(7)	2.262(19)	O(3)–Zn(1)–N(1)	85.5(6)	N(7)–Zn(2)–O(11)	94.6(8)
Zn(2)–O(12)	2.294(19)	O(4)–Zn(1)–N(1)	89.0(6)	O(12)–Zn(2)–O(11)	93.1(9)
Zn(2)–O(10)	2.299(15)	O(5)–Zn(1)–N(1)	91.8(5)	O(10)–Zn(2)–O(11)	88.4(8)
Zn(2)–O(11)	2.37(2)	N(2) <sup>a</sup> –Zn(1)–O(6)	88.9(6)	N(8) <sup>a</sup> –Zn(2)–O(9)	81.8(9)
Zn(2)–O(9)	2.42(2)	O(3)–Zn(1)–O(6)	84.3(7)	N(7)–Zn(2)–O(9)	92.4(8)
		O(4)–Zn(1)–O(6)	177.3(7)	O(12)–Zn(2)–O(9)	81.7(9)
		O(5)–Zn(1)–O(6)	86.5(7)	O(10)–Zn(2)–O(9)	96.0(7)
		N(1)–Zn(1)–O(6)	92.6(6)	O(11)–Zn(2)–O(9)	171.5(7)
2					
Cd(1)–O(5)	2.282(13)	O(5)–Cd(1)–O(4)	85.5(5)	O(11)–Cd(2)–N(7)	95.0(4)
Cd(1)–O(4)	2.281(11)	O(5)–Cd(1)–N(1)	92.5(4)	O(11)–Cd(2)–O(10)	88.1(6)
Cd(1)–N(1)	2.320(8)	O(4)–Cd(1)–N(1)	89.4(4)	N(7)–Cd(2)–O(10)	92.7(4)
Cd(1)–N(2) <sup>b</sup>	2.321(9)	O(5)–Cd(1)–N(2) <sup>b</sup>	87.0(4)	O(11)–Cd(2)–N(8) <sup>a</sup>	88.2(5)
Cd(1)–O(3)	2.329(11)	O(4)–Cd(1)–N(2) <sup>b</sup>	91.3(3)	N(7)–Cd(2)–N(8) <sup>a</sup>	176.6(6)
Cd(1)–O(6)	2.343(9)	N(1)–Cd(1)–N(2) <sup>b</sup>	179.1(4)	O(10)–Cd(2)–N(8) <sup>a</sup>	88.5(4)
Cd(2)–O(11)	2.230(14)	O(5)–Cd(1)–O(3)	172.2(4)	O(11)–Cd(2)–O(9)	93.3(5)
Cd(2)–N(7)	2.256(9)	O(4)–Cd(1)–O(3)	86.9(4)	N(7)–Cd(2)–O(9)	91.5(3)
Cd(2)–O(10)	2.288(10)	N(1)–Cd(1)–O(3)	88.9(3)	O(10)–Cd(2)–O(9)	175.4(4)
Cd(2)–N(8) <sup>a</sup>	2.302(10)	N(2) <sup>b</sup> –Cd(1)–O(3)	91.7(3)	N(8) <sup>a</sup> –Cd(2)–O(9)	87.2(4)
Cd(2)–O(9)	2.340(8)	O(5)–Cd(1)–O(6)	93.0(4)	O(11)–Cd(2)–O(12)	167.9(4)
Cd(2)–O(12)	2.401(11)	O(4)–Cd(1)–O(6)	178.4(5)	N(7)–Cd(2)–O(12)	93.1(4)
		N(1)–Cd(1)–O(6)	91.1(3)	O(10)–Cd(2)–O(12)	82.4(5)
		N(2) <sup>b</sup> –Cd(1)–O(6)	88.1(3)	N(8) <sup>a</sup> –Cd(2)–O(12)	84.0(5)
		O(3)–Cd(1)–O(6)	94.6(3)	O(9)–Cd(2)–O(12)	95.5(4)
3					
Cd(1)–N(1)	2.268(9)	N(1)–Cd(1)–N(2) <sup>c</sup>	169.3(4)	N(3)–Cd(2)–O(19)	106.8(10)
Cd(1)–N(2) <sup>c</sup>	2.281(10)	N(1)–Cd(1)–O(3)	88.1(5)	N(4) <sup>d</sup> –Cd(2)–O(19)	85.7(10)
Cd(1)–O(3)	2.304(18)	N(2) <sup>c</sup> –Cd(1)–O(3)	86.7(5)	O(16)–Cd(2)–O(2)	124.6(11)
Cd(1)–O(8)	2.389(17)	N(1)–Cd(1)–O(8)	97.5(5)	N(3)–Cd(2)–O(2)	83.8(4)
Cd(1)–O(1)	2.368(16)	N(2) <sup>c</sup> –Cd(1)–O(8)	90.7(5)	N(4) <sup>d</sup> –Cd(2)–O(2)	83.4(4)
Cd(1)–O(18)	2.43(2)	O(3)–Cd(1)–O(8)	79.6(6)	O(19)–Cd(2)–O(2)	165.9(11)
Cd(1)–O(10)	2.488(11)	N(1)–Cd(1)–O(1)	97.8(6)	O(16)–Cd(2)–O(4)	105.0(9)
Cd(2)–O(16)	2.258(14)	N(2) <sup>c</sup> –Cd(1)–O(1)	92.6(6)	N(3)–Cd(2)–O(4)	93.0(4)
Cd(2)–N(3)	2.287(10)	O(3)–Cd(1)–O(1)	132.3(7)	N(4) <sup>d</sup> –Cd(2)–O(4)	96.0(4)
Cd(2)–N(4) <sup>d</sup>	2.289(10)	O(8)–Cd(1)–O(1)	52.7(7)	O(19)–Cd(2)–O(4)	59.9(9)
Cd(2)–O(19)	2.82(4)	N(1)–Cd(1)–O(18)	92.2(7)	O(2)–Cd(2)–O(4)	130.2(7)
Cd(2)–O(2)	2.42(2)	N(2) <sup>c</sup> –Cd(1)–O(18)	88.3(6)	O(16)–Cd(2)–O(7)	155.5(9)
Cd(2)–O(4)	2.44(11)	O(3)–Cd(1)–O(18)	153.2(6)	N(3)–Cd(2)–O(7)	86.9(4)
Cd(2)–O(7)	2.514(11)	O(8)–Cd(1)–O(18)	126.8(7)	N(4) <sup>d</sup> –Cd(2)–O(7)	91.7(4)
Cd(2)–O(17)	2.51(3)	O(1)–Cd(1)–O(18)	74.2(8)	O(19)–Cd(2)–O(7)	110.1(9)
		N(1)–Cd(1)–O(10)	90.0(4)	O(2)–Cd(2)–O(7)	79.2(7)
		N(2) <sup>c</sup> –Cd(1)–O(10)	79.4(4)	O(4)–Cd(2)–O(7)	51.0(4)
		O(3)–Cd(1)–O(10)	53.5(5)	O(16)–Cd(2)–O(17)	49.9(10)
		O(8)–Cd(1)–O(10)	132.3(6)	N(3)–Cd(2)–O(17))	90.9(7)
		O(1)–Cd(1)–O(10)	170.2(6)	N(4) <sup>d</sup> –Cd(2)–O(17)	84.8(7)
		O(18)–Cd(1)–O(10)	99.7(6)	O(19)–Cd(2)–O(17)	94.9(10)
		O(16)–Cd(2)–N(3)	90.0(5)	O(2)–Cd(2)–O(17)	75.2(9)
		O(16)–Cd(2)–N(4) <sup>d</sup>	96.4(6)	O(4)–Cd(2)–O(17)	154.6(8)
		N(3)–Cd(2)–N(4) <sup>d</sup>	167.2(4)	O(7)–Cd(2)–O(17)	154.4(7)
		O(16)–Cd(2)–O(19)	47.9(7)		
4					
Cd(1)–N(4)	2.280(11)	N(4)–Cd(1)–N(2)	92.9(4)	O(13)–Cd(1)–N(3) <sup>f</sup>	89.2(4)
Cd(1)–N(2)	2.324(9)	N(4)–Cd(1)–N(1) <sup>e</sup>	90.9(4)	N(7)–Cd(2)–N(8) <sup>g</sup>	87.4(3)
Cd(1)–N(1) <sup>e</sup>	2.333(10)	N(2)–Cd(1)–N(1) <sup>e</sup>	173.9(4)	N(7)–Cd(2)–N(9) <sup>h</sup>	173.1(4)
Cd(1)–O(7)	2.343(11)	N(4)–Cd(1)–O(7)	92.2(4)	N(8) <sup>g</sup> –Cd(2)–N(9) <sup>h</sup>	91.6(3)
Cd(1)–O(13)	2.344(9)	N(2)–Cd(1)–O(7)	85.4(4)	N(7)–Cd(2)–O(16)	89.7(3)
Cd(1)–N(3) <sup>f</sup>	2.350(11)	N(1) <sup>e</sup> –Cd(1)–O(7)	89.8(4)	N(8) <sup>f</sup> –Cd(2)–O(16)	87.7(3)
Cd(2)–N(7)	2.307(10)	N(4)–Cd(1)–O(13)	86.0(4)	N(9) <sup>h</sup> –Cd(2)–O(16)	83.5(3)
Cd(2)–N(8) <sup>g</sup>	2.322(10)	N(2)–Cd(1)–O(13)	95.1(3)	N(7)–Cd(2)–N(5)	90.5(3)
Cd(2)–N(9) <sup>h</sup>	2.330(9)	N(1) <sup>e</sup> –Cd(1)–O(13)	89.9(3)	N(8) <sup>g</sup> –Cd(2)–N(5)	177.3(3)
Cd(2)–O(16)	2.346(8)	O(7)–Cd(1)–O(13)	178.2(4)	N(9) <sup>h</sup> –Cd(2)–N(5)	90.6(3)
Cd(2)–N(5)	2.351(9)	N(4)–Cd(1)–N(3) <sup>f</sup>	175.1(5)	O(16)–Cd(2)–N(5)	94.0(3)
Cd(2)–O(2)	2.402(9)	N(2)–Cd(1)–N(3) <sup>f</sup>	86.2(3)	N(7)–Cd(2)–O(2)	86.0(3)
		N(1) <sup>e</sup> –Cd(1)–N(3) <sup>f</sup>	90.4(4)	N(8) <sup>g</sup> –Cd(2)–O(2)	92.3(3)
		O(7)–Cd(1)–N(3) <sup>f</sup>	92.6(4)	N(9) <sup>h</sup> –Cd(2)–O(2)	100.8(3)

**Table 2.** (Continued)

Cd(1)–N(6) <sup>j</sup>	2.340(9)	N(6) <sup>i</sup> –Cd(1)–N(6) <sup>j</sup>	102.6(6)	N(2) <sup>j</sup> –Cd(2)–N(2) <sup>j</sup>	88.8(4)
Cd(1)–N(3)	2.345(13)	N(6) <sup>i</sup> –Cd(1)–N(3)	86.4(4)	N(2) <sup>j</sup> –Cd(2)–N(5)	88.5(3)
Cd(1)–O(1)	2.489(8)	N(6) <sup>i</sup> –Cd(1)–N(3)	163.9(4)	N(2) <sup>j</sup> –Cd(2)–N(5)	170.7(4)
Cd(2)–N(2) <sup>j</sup>	2.349(9)	N(3)–Cd(1)–N(3) <sup>k</sup>	88.2(6)	N(5)–Cd(2)–N(5) <sup>m</sup>	95.5(4)
Cd(2)–N(5)	2.354(9)	N(6) <sup>i</sup> –Cd(1)–O(1)	75.7(3)	N(2) <sup>j</sup> –Cd(2)–O(8) <sup>m</sup>	84.9(4)
Cd(2)–O(8)	2.401(12)	N(6) <sup>i</sup> –Cd(1)–O(1)	82.6(3)	N(5)–Cd(2)–O(8) <sup>m</sup>	86.1(3)
		N(3)–Cd(1)–O(1)	86.9(3)	N(2) <sup>j</sup> –Cd(2)–O(8)	84.9(4)
		N(6) <sup>i</sup> –Cd(1)–O(1) <sup>k</sup>	75.7(3)	N(2) <sup>j</sup> –Cd(2)–O(8)	86.3(5)
		N(3)–Cd(1)–O(1) <sup>k</sup>	119.1(4)	N(5)–Cd(2)–O(8)	102.3(5)
		O(1)–Cd(1)–O(1) <sup>k</sup>	145.0(3)	O(8) <sup>m</sup> –Cd(2)–O(8)	167.6(6)
<b>6</b>					
Ni(1)–N(1) <sup>n</sup>	2.112(9)	N(1) <sup>n</sup> –Ni(1)–N(1) <sup>o</sup>	90.4(5)	N(2)–Ni(1)–Cl(4) <sup>p</sup>	89.9(3)
Ni(1)–N(2)	2.141(9)	N(1) <sup>n</sup> –Ni(1)–N(2)	89.0(3)	N(3) <sup>q</sup> –Ni(2)–N(4) <sup>r</sup>	89.5(4)
Ni(1)–Cl(4)	2.434(3)	N(1) <sup>o</sup> –Ni(1)–N(2)	178.8(4)	N(3)–Ni(2)–N(4) <sup>r</sup>	176.3(4)
Ni(2)–N(3)	2.099(10)	N(2) <sup>p</sup> –Ni(1)–N(2)	91.6(5)	N(4) <sup>u</sup> –Ni(2)–N(4) <sup>s</sup>	86.9(6)
Ni(2)–N(4) <sup>r</sup>	2.134(11)	N(1) <sup>n</sup> –Ni(1)–Cl(4)	91.2(3)	N(3)–Ni(2)–Cl(1)	88.2(3)
Ni(2)–Cl(1)	2.467(4)	N(1) <sup>o</sup> –Ni(1)–Cl(4)	91.1(3)	N(4) <sup>u</sup> –Ni(2)–Cl(1)	91.0(4)
		N(2)–Ni(1)–Cl(4)	87.9(3)	N(3)–Ni(2)–Cl(1) <sup>q</sup>	89.5(3)
		Cl(4)–Ni(1)–Cl(4) <sup>p</sup>	176.8(2)	N(4) <sup>u</sup> –Ni(2)–Cl(1) <sup>q</sup>	91.4(4)
		N(3) <sup>q</sup> –Ni(2)–N(3)	94.1(5)	Cl(1)–Ni(2)–Cl(1) <sup>q</sup>	176.7(2)

<sup>a</sup> Symmetry transformations used to generate equivalent atoms: <sup>a</sup>x – 1, y – 1, z + 1; <sup>b</sup>x + 1, y + 1, z – 1; <sup>c</sup>x, y, z + 1; <sup>d</sup>x, y, z – 1; <sup>e</sup>x – 1, y + 1, z; <sup>f</sup>x + 1, y, z – 1; <sup>g</sup>x – 1, y, z + 1; <sup>h</sup>x + 1, y – 1, z; <sup>i</sup>–x + 3/2, y – 1/2, –z + 2; <sup>j</sup>x + 1/2, y – 1/2, z – 1; <sup>k</sup>–x + 2, y, –z + 1; <sup>l</sup>–x + 1/2, y – 1/2, –z + 1; <sup>m</sup>–x + 1, y, –z; <sup>n</sup>–x + 3/2, y + 1/2, –z; <sup>o</sup>x – 1/2, y + 1/2, z + 1; <sup>p</sup>–x + 1, y, –z + 1; <sup>q</sup>–x + 1, y, –z + 2; <sup>r</sup>x – 1/2, y – 1/2, z + 1; <sup>s</sup>–x + 3/2, y – 1/2, –z + 1.

**Scheme 1**

**X-ray Structure Determinations.** The determinations of the unit cells and data collections for all crystals of compounds **1–6** were performed on a Siemens SMART CCD. The data were collected using graphite-monochromatic Mo K $\alpha$  radiation ( $\lambda = 0.710\text{73}\text{\AA}$ ) at 173 K. The data sets were corrected by the SADABS program.<sup>16</sup> All structures were solved by direct methods and refined by full-matrix least-squares methods with the SHELXTL-97 program package.<sup>17</sup> Crystallographic data are summarized in Table 1 and the selected bond lengths and angles listed in Table 2 (see also the Supporting Information).

## Results and Discussion

The new enantiopure ligand 6,6'-dichloro-2,2'-diethoxy-1,1'-binaphthyl-4,4'-bis(vinylpyridine) (**L**) was obtained via a Pd-catalyzed Heck coupling reaction between 6,6'-dichloro-4,4'-dibromo-2,2'-diethoxy-1,1'-binaphthyl<sup>18</sup> and 4-vinylpyridine in 74% yield (Scheme 1). The new ligand **L** was characterized by  $^1\text{H}$  and  $^{13}\text{C}\{^1\text{H}\}$  NMR spectroscopy.

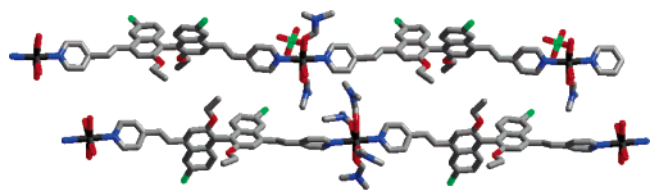


**Figure 1.** A view of the two different 1D polymeric chains in **1**. The black, green, red, blue, and gray colors represent Zn, Cl, O, N, and C atoms, respectively.

The slow diffusion of diethyl ether into a mixture of zinc perchlorate and ligand **L** in DMF/CHCl<sub>3</sub>/EtOH gave colorless crystals of [ZnL(DMF)<sub>4</sub>][ZnL(DMF)<sub>2</sub>(H<sub>2</sub>O)(ClO<sub>4</sub>)<sub>2</sub>](ClO<sub>4</sub>)<sub>3</sub>·2DMF·EtOH·2H<sub>2</sub>O (**1**) in 41.7% yield. Compound **1** crystallizes in the *P*1 space group with two Zn(II) centers and two **L** ligands in the asymmetric unit. The first Zn(II) center adopts a distorted octahedral environment by coordinating to four DMF molecules (Zn–O = 2.291–2.362 Å) in the equatorial positions and to two pyridines from two different **L** ligands in the axial positions (Zn–N = 2.278–2.363 Å). The second octahedrally coordinated Zn(II) center binds to two DMF (Zn–O = 2.294–2.299 Å), one water (Zn–O = 2.368 Å), and one perchlorate group (Zn–O = 2.419 Å) in the equatorial positions and to two pyridines of two different **L** ligands in the axial positions (Zn–N = 2.213–2.262 Å). The Zn(II) centers are linked to each other by the **L** ligands and propagate into an infinite 1D coordination polymer with the formula of [ZnL(DMF)<sub>4</sub>] and [ZnL(DMF)<sub>2</sub>(H<sub>2</sub>O)(ClO<sub>4</sub>)<sub>2</sub>], respectively (Figure 1). The dihedral angles of the two independent binaphthyl subunits in **1** are 79.6° and 61.7°, respectively. The neighboring chains interact with each other via  $\pi$ ··· $\pi$  interactions (the nearest C–C distance is 3.314 Å) to lead to small 1D chiral channels (3.744 × 7.591 Å<sup>2</sup>) along the *a* axis. On the basis of PLATON calculations,<sup>19</sup>

(16) Sheldrick, G. M. *SADABS, Absorption Correction Program*; University of Göttingen: Göttingen, Germany, 1996.

(17) Sheldrick, G. M. *Program for Structure Refinement*; University of Göttingen: Göttingen, Germany, 1997.

(18) Lee, S. J.; Lin, W. *J. Am. Chem. Soc.* **2002**, *124*, 4554.

(19) Spek, A. L. *PLATON, A Multipurpose Crystallographic Tool*; Utrecht University: Utrecht, The Netherlands, 2001.

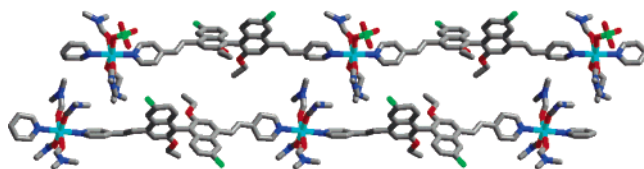


**Figure 2.** A view of the two different 1D polymeric chains in **2**. The cyan, green, red, blue, and gray colors represent Zn, Cl, O, N, and C atoms, respectively.

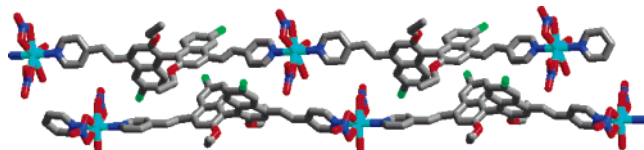


**Figure 3.** A view of the two different 1D polymeric chains in **3**. The cyan, green, red, blue, and gray colors represent Zn, Cl, O, N, and C atoms, respectively.

the open channels constitute about 27.7% ( $832.4 \text{ \AA}^3$  out of  $3002.2 \text{ \AA}^3$ ) of the crystal volume and are filled with  $\text{ClO}_4^-$  anions and noncoordinating DMF, EtOH, and  $\text{H}_2\text{O}$  molecules. TGA showed that **1** lost 9.3% of its total weight in the 20–130 °C temperature range, corresponding to the loss of noncoordinating solvents (expected 9.3% for two water, one EtOH, and two DMF molecules per formula unit).

$[\text{CdL}(\text{DMF})_4][\text{CdL}(\text{DMF})_3(\text{ClO}_4)] \cdot (\text{ClO}_4)_3 \cdot 2\text{DMF}$  (**2**) was synthesized in a similar fashion to **1**. Compound **2** also crystallizes in the *P*1 space group with a very similar 1D chain structure as that of **1** (Figure 2). The second Cd(II) center in **2** has a slightly different coordination environment with the equatorial positions occupied by three DMF and one perchlorate group. The dihedral angles of the two independent binaphthyl subunits in **2** are 80.5° and 61.6°. The network structure of **2** is stabilized by strong  $\pi \cdots \pi$  interactions between naphthyl rings and vinyl groups of neighboring **L** ligands (the nearest C–C separation is 3.319 Å). The void space in **2** accounts for 24.0% of the crystal volume and is filled with  $\text{ClO}_4^-$  anions and DMF solvent molecules. TGA analysis showed that **2** lost 5.9% of its total weight in the 20–85 °C temperature range, corresponding to the loss of two DMF molecules per formula unit (expected 5.8%). Compound **2** loses the coordinated DMF molecules upon further heating.

Colorless crystals of  $[\text{CdL}(\text{H}_2\text{O})(\text{NO}_3)_2][\text{CdL}(\text{H}_2\text{O})_2(\text{NO}_3)_2] \cdot \text{MeOH}$  (**3**) were obtained by heating a mixture of  $\text{Cd}(\text{NO}_3)_2 \cdot 4\text{H}_2\text{O}$  and **L** in *o*- $\text{C}_6\text{H}_4\text{Cl}_2$ /MeOH in a capped vial at 70 °C for 1 week. Compound **3** adopts a similar 1D polymeric chain structure (space group *P*2<sub>1</sub>) as that of **2** except that both crystallographically independent Cd(II) centers in **3** adopt seven-coordinate environments (Figure 3). One Cd atom coordinates to two bidentate nitrates (Cd–O = 2.304–2.488 Å), one aqua ligand (Cd–O = 2.426 Å), and two pyridines of two different **L** ligands (Cd–N = 2.268–2.281 Å), while the other Cd atom coordinates to one bidentate nitrate (Cd–O = 2.441–2.514 Å), one monodentate nitrate (Cd–O = 2.258 Å), two water molecules (Cd–O = 2.415–2.513 Å), and two pyridines of two different **L** ligands (Cd–N = 2.287–2.289 Å). The coordination of two nitrate anions to each Cd(II) center in **3** leads to a neutral

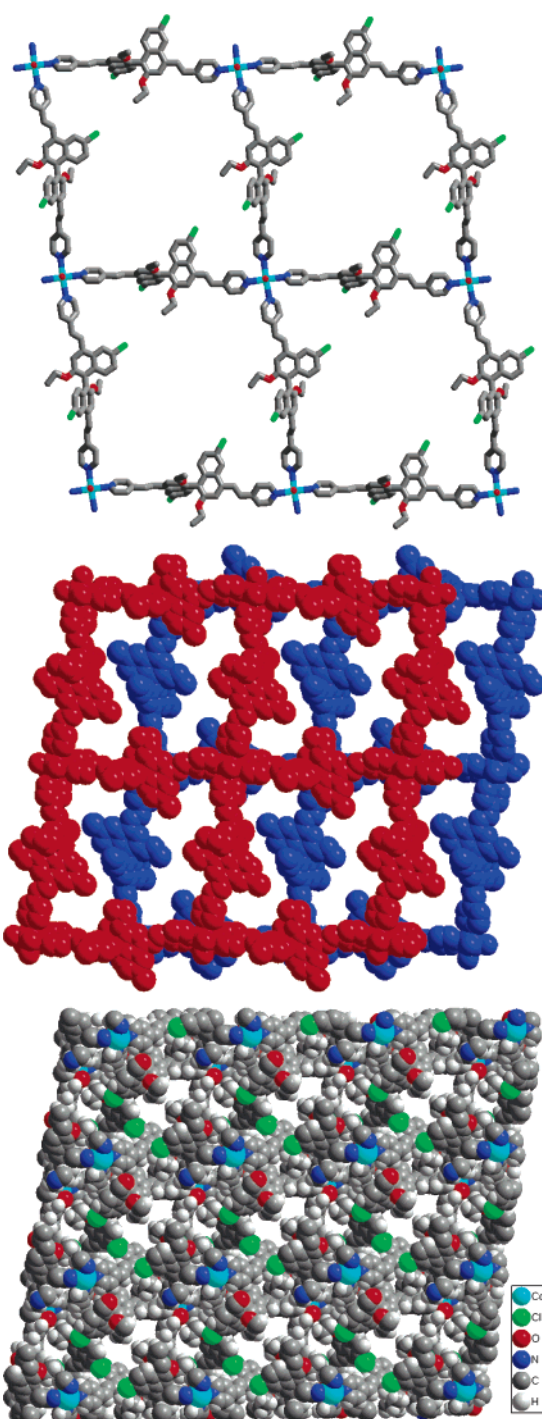


**Figure 4.** A view of one of the two 2D lamellar frameworks of **4** (top). A view of the AB stacking mode of the rhombic grids in **4** (middle). A space-filling view of **4** as along the *a* axis showing two different channels of  $9.7 \times 10.2$  and  $6.7 \times 7.7 \text{ \AA}^2$  in size (bottom).

1D polymeric chain structure, and as a consequence, the accessible void space in **3** is much smaller and can only accommodate one MeOH molecule in each formula unit. TGA analysis showed that **3** lost 1.2% of its total weight in the 20–68 °C temperature range, corresponding to the loss of one MeOH molecule per formula unit (expected 1.2%).

When EtOH was replaced by acetonitrile during the synthesis of **2**,  $[\text{CdL}_2(\text{H}_2\text{O})(\text{DMF})][\text{CdL}_2(\text{H}_2\text{O})(\text{ClO}_4)](\text{ClO}_4)_3 \cdot \text{DMF} \cdot 3\text{CH}_3\text{CN} \cdot 6\text{H}_2\text{O}$  (**4**) with a very different network

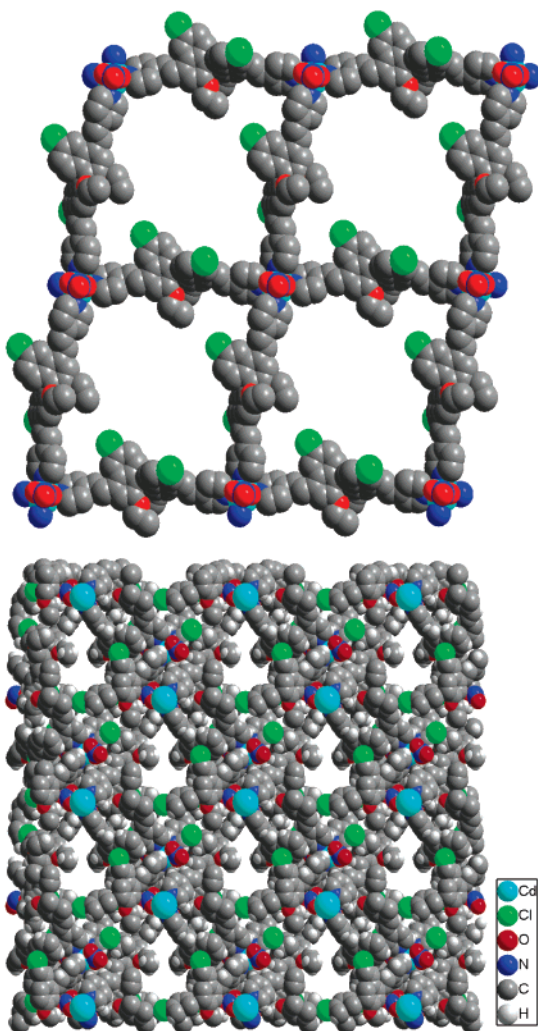


**Figure 5.** A view of the 2D lamellar frameworks of **5** (top). A space-filling view of **5** down the *c* axis (bottom).

structure was obtained as colorless crystals. Compound **4** crystallizes in the *P*1 space group with two unique Cd(II) centers in the asymmetric unit. Each of the two independent Cd atoms coordinates to four pyridines of four different **L** ligands and one aqua ligand. For the sixth coordination site, one Cd coordinates to one DMF molecule ( $\text{Cd}-\text{O} = 2.344 \text{ \AA}$ ) while the other Cd coordinates to one perchlorate anion ( $\text{Cd}-\text{O} = 2.402 \text{ \AA}$ ). Each of the two independent Cd atoms is propagated by the **L** ligands to form crystallographically independent lamellar structures that are built from coordination rhombuses of  $24.705 \times 24.750 \text{ \AA}^2$  in size (Figure 4). The dihedral angles of the four independent binaphthyl subunits in **4** are  $68.5^\circ$ ,  $82.0^\circ$ ,  $79.1^\circ$ , and  $69.4^\circ$ . The neighboring rhombic grids stack together in an  $\cdots\text{ABAB}\cdots$  fashion, which are stabilized by strong  $\pi\cdots\pi$  interactions (the nearest  $\text{C}\cdots\text{C}$  distance is  $3.306 \text{ \AA}$ ) between adjacent naphthyl rings of the neighboring lamellae. Compound **4** possesses two different channels ( $9.7 \times 10.2 \text{ \AA}^2$  and  $6.7 \times 7.7 \text{ \AA}^2$ ) along the *a* axis. Calculations using PLATON reveal that the open channels constitute about 34.3% ( $1582.1 \text{ \AA}^3$  out of  $4616.0 \text{ \AA}^3$ ) of the crystal volume and are filled with  $\text{ClO}_4^-$  anions, DMF,  $\text{CH}_3\text{CN}$ , and  $\text{H}_2\text{O}$  solvent molecules. TGA

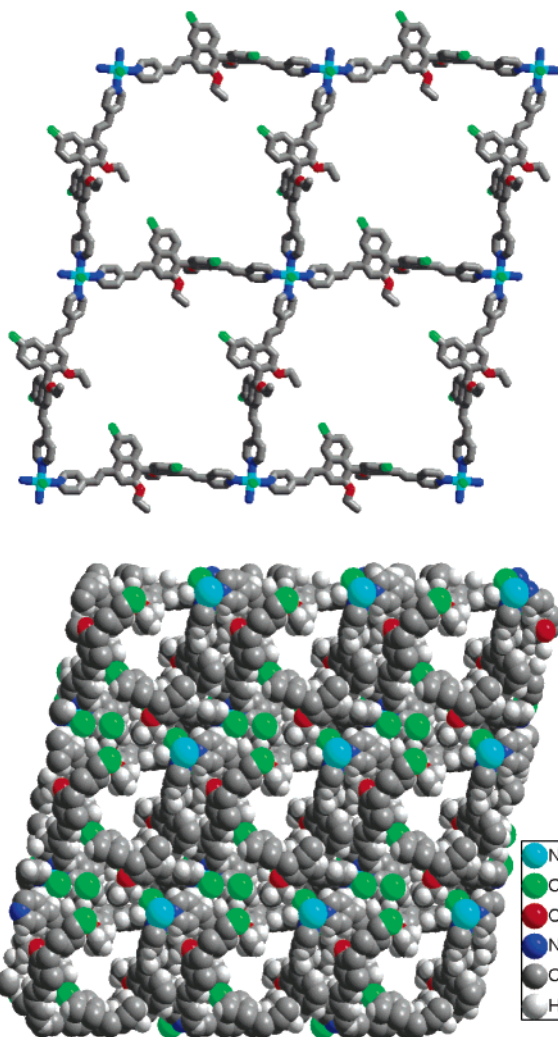


**Figure 6.** A view of 2D rhombic grids in **6** (top). A space-filling view of **6** down the *c* axis (bottom).

analysis showed that **4** lost 8.6% of its total weight in the  $20\text{--}190^\circ\text{C}$  temperature range, corresponding to the loss of all solvent molecules (expected 8.5%).

Single crystals of  $[\text{CdL}_2(\text{NO}_3)_2]\cdot\text{DMF}\cdot2\text{EtOH}\cdot2.5\text{H}_2\text{O}$  (**5**) were grown by the slow diffusion of diethyl ether into a mixture of **L** and  $\text{Cd}(\text{NO}_3)_2\cdot4\text{H}_2\text{O}$  in ethyl acetate and DMF for 4 days. Compound **5** crystallizes in space group *C*2. The Cd(II) centers in **5** adopt distorted octahedral environments with four pyridyl groups at the equatorial positions [ $\text{Cd}-\text{N} = 2.340(9)\text{--}2.354(9) \text{ \AA}$ ] and two monodentate nitrate groups at the apical positions [ $\text{Cd}-\text{O} = 2.401(12)\text{--}2.489(8) \text{ \AA}$ ]. As depicted in Figure 5, the Cd(II) ions are linked by the **L** ligands to yield rhombic grids of  $24.831 \times 24.831 \text{ \AA}^2$  in dimension. Adjacent 2D grids stack along the *c* axis with an offset of  $0.5a + 0.252b$  along the *ab* plane and are shifted by  $0.5c$  along the *c* axis. These grids thus stack in an  $\cdots\text{ABAB}\cdots$  fashion with significant offsets in the *ab* plane to leave open channels of  $11.392 \times 16.497 \text{ \AA}^2$  along the *c* axis (Figure 5b). The solvent-accessible volume calculated with the PLATON program is  $2600.0 \text{ \AA}^3$  (29.6% of the unit cell volume). TGA analysis indicated a weight loss of 12.4% at  $20\text{--}135^\circ\text{C}$ , corresponding to the loss of solvent molecules (expected 12.5%).

Compound **5** lost all of the solvent molecules after it was ground and heated at 50 °C for 12 h under a vacuum. The resulting powder showed sharp X-ray diffraction peaks similar to those of the pristine sample. This result indicates that the two-dimensional metal-organic framework structure of **5** is retained after the removal of all of the solvent molecules.

$[\text{NiL}_2\text{Cl}_2]\cdot\text{DMF}\cdot4\text{EtOH}\cdot\text{H}_2\text{O}$  (**6**) was prepared by the slow diffusion of  $\text{Et}_2\text{O}$  into a mixture of  $\text{NiCl}_2\cdot6\text{H}_2\text{O}$  and **L** in a mixed solvent of DMF,  $\text{CHCl}_3$ , and EtOH. Compound **6** is isostructural to **5** with the Ni(II) center octahedrally coordinated to four pyridines of four different **L** ligands ( $\text{Ni}-\text{N} = 2.099\text{--}2.141 \text{ \AA}$ ) and two chloride atoms ( $\text{Ni}-\text{Cl} = 2.434\text{--}2.467 \text{ \AA}$ ) (Figure 6). Adjacent 2D grids in **6** stack along the *c* axis with an offset of  $a + 0.243b$  along the *ab* plane and are shifted by  $0.5c$  along the *c* axis. These grids thus stack in an  $\cdots\text{ABAB}\cdots$  fashion with significant offsets in the *ab* plane to leave open channels of  $12.207 \times 16.417 \text{ \AA}^2$  along the *c* axis. The neighboring lamellae are held together by strong  $\pi\cdots\pi$  edge interactions (the nearest C $\cdots$ C distance of neighboring molecules is 3.258 Å) and  $\pi\cdots\pi$  interactions (the nearest C $\cdots$ C distance of neighboring molecules is 3.396 Å). The effective pore volume for inclusion in **6** is  $3252.9 \text{ \AA}^3$  per unit cell (35.8% of the crystal volume), and TGA analysis showed that **6** lost all of the solvent molecules by 103 °C (calcd, 16.8%; found, 16.7%).

## Summary

We have utilized a chiral binaphthyl-derived 4,4'-bipyridine-based bridging ligand for the synthesis of six homochiral metal-organic frameworks. Two polymeric motifs were

observed in these compounds: the one-dimensional polymeric structure with bridging ligands occupying the axial positions of the metal centers and two-dimensional rhombic grids formed by the linking of octahedrally coordinated metal centers with four pyridyl ligands in the equatorial positions. As the bridging ligands are long, compounds **4**–**6** adopt  $\cdots\text{ABAB}\cdots$  offset stacking modes to reduce the potentially very large void space. Our findings can be generalized as follows: (1) The formation of distinct topological architectures is affected by the solvents used in the crystal growth. (2) The counterions can have a very significant influence on the formation of MOFs, even when most of the anions only occupy the void spaces of the open frameworks. (3) The nature of metal ions, because of their different coordination environments, plays critical roles in the formation of MOFs with different architectures. With the knowledge of synthesizing a large variety of chiral porous MOFs, we are well-poised to incorporate desired functional groups in the chiral bridging ligands for the synthesis of catalytically active materials.

**Acknowledgment.** We thank NSF (CHE-0512495) for financial support. W.L. is a Camille Dreyfus Teacher-Scholar.

**Supporting Information Available:** Crystallographic information in CIF format; a table of bond lengths and angles for compounds 1–6; and figures of packing diagrams, stacking modes, IR spectra, TGA curves, and powder X-ray diffraction patterns. This material is available free of charge via the Internet at <http://pubs.acs.org>.

IC060891X